PLOS GENETICS

RESEARCH ARTICLE

Forward genetic screen of homeostatic antibody levels in the Collaborative Cross identifies MBD1 as a novel regulator of B cell homeostasis

Brea K. Hampton[1,2], Kenneth S. Plante[2], Alan C. Whitmore[2], Colton L. Linnertz[2], Emily A. Madden[3], Kelsey E. Noll[3], Samuel P. Boyson[1,2], Breantie Parotti[2], James G. Xenakis[2], Timothy A. Bell[2], Pablo Hock[2], Ginger D. Shaw[2], Fernando Pardo-Manuel de Villena[2,4], Martin T. Ferris[2]*, Mark T. Heise[2,3,4]*

1 Curriculum in Genetics and Molecular Biology, University of North Carolina at Chapel Hill, Chapel Hill, North Carolina, United States of America, **2** Department of Genetics, University of North Carolina at Chapel Hill, Chapel Hill, North Carolina, United States of America, **3** Department of Microbiology and Immunology, University of North Carolina at Chapel Hill, Chapel Hill, North Carolina, United States of America, **4** Lineberger Comprehensive Cancer Center, University of North Carolina, Chapel Hill, North Carolina, United States of America

* mtferris@email.unc.edu (MTF); mark_heisem@med.unc.edu (MTH)

Citation: Hampton BK, Plante KS, Whitmore AC, Linnertz CL, Madden EA, Noll KE, et al. (2022) Forward genetic screen of homeostatic antibody levels in the Collaborative Cross identifies MBD1 as a novel regulator of B cell homeostasis. PLoS Genet 18(12): e1010548. https://doi.org/10.1371/journal.pgen.1010548

Editor: Ryan A. Langlois, University of Minnesota, UNITED STATES

Received: September 2, 2022

Accepted: November 28, 2022

Published: December 27, 2022

Data Availability Statement: All relevant data are within the manuscript and its Supporting Information files.

Funding: This work was supported, in part, by U19AI100625 (to MTH, MTF, and FPMV), P01AI132130 (to FPMV and MTF), R21AI119933 (to MTH), HHMI Gilliam Fellowship (to BKH), and F99AG073570 (to BKH). The funders had no role in study design, data collection and analysis, decision to publish, or preparation of the manuscript.

Abstract

Variation in immune homeostasis, the state in which the immune system is maintained in the absence of stimulation, is highly variable across populations. This variation is attributed to both genetic and environmental factors. However, the identity and function of specific regulators have been difficult to identify in humans. We evaluated homeostatic antibody levels in the serum of the Collaborative Cross (CC) mouse genetic reference population. We found heritable variation in all antibody isotypes and subtypes measured. We identified 4 quantitative trait loci (QTL) associated with 3 IgG subtypes: IgG1, IgG2b, and IgG2c. While 3 of these QTL map to genome regions of known immunological significance (major histocompatibility and immunoglobulin heavy chain locus), *Qih1* (associated with variation in IgG1) mapped to a novel locus on Chromosome 18. We further associated this locus with B cell proportions in the spleen and identify Methyl-CpG binding domain protein 1 under this locus as a novel regulator of homeostatic IgG1 levels in the serum and marginal zone B cells (MZB) in the spleen, consistent with a role in MZB differentiation to antibody secreting cells.

Author summary

The baseline immune state is highly variable across populations, which is a function of both environmental and genetics factors. Here, we have used the Collaborative Cross, a genetically diverse mouse population, to study the role of genetic variation on baseline serum antibody concentrations. We identified several regions of the genome that were associated with variation in serum concentrations of multiple antibody subtypes. Most of which are in regions of the genome that have been shown previously to impact immune

Competing interests: The authors have declared that no competing interests exist.

responses. We also identified a novel region of the genome associated with variation in IgG1 and further identify Methyl-CpG binding domain protein 1 (MBD1) as a regulator of both baseline IgG1 and B cell homeostasis. Given that MBD1 is an epigenetic regulator of differentiation in other contexts, further studies of MBD1 in B cell homeostasis may define previously unknown pathways involved in marginal zone B cell differentiation.

Introduction

Immune homeostasis is the stable state that the immune system maintains in the absence of insult. While the majority of studies on host immunity have focused on the response to specific stimuli (e.g., pathogens, vaccines, allergens, or adjuvants), a growing body of evidence suggests that an individual's baseline immune status affects subsequent innate or antigen specific immune responses [1–4]. Immune homeostatic parameters are gaining increasing recognition as predictors of clinical outcomes to immunotherapy and vaccination [1,3], and several studies have shown that dysregulation of immune homeostasis can contribute to the development of cancer, autoimmunity, allergies, as well as the progression of immune-related pathology in response to infection [5]. Natural antibodies, which are present before antigen exposure, are a major component of immune homeostasis. These antibodies have been shown to be produced by specific subsets of B cells (e.g., marginal zone B cells and B1 B cells) and provide a first line of defense against infection through low affinity binding to pathogens [6]. Concurrent with our understanding of B cell and antibody biology, there is growing evidence that immune homeostasis is under genetic control [7–10]. However, we still do not fully understand the role that genetic differences between individuals play in driving baseline immunity.

Many studies have shown that humans exhibit significant inter-individual variation in baseline immune phenotypes [3–4,11–12]. However, it has been difficult to identify the genes that contribute to this variation due to a variety of confounding factors. These include difficult to control environmental factors, such as prior microbial and environmental exposures as well as age- dependent changes in immune status that create a highly dynamic immune environment [13]. Rodent models, which allow for greater control of host genetics and environmental exposures, represent an attractive system with which to model and investigate those factors driving the development of various immune homeostatic states. Gene specific knockout mice have been critical to our understanding of the immune system. However, these models represent extreme genetic perturbations, rather than the more subtle effects on gene expression or function more commonly associated with naturally occurring genetic variation in humans.

To better model how natural genetic variation impacts immune homeostasis, we turned to the Collaborative Cross (CC) genetic reference panel (grp) [14]. The CC grp is a large set of recombinant inbred (RI) mouse strains derived from 8 founders: five classical laboratory strains (C57BL/6J (B6), A/J, 129S1/SvImJ (129S1), NOD/ShiLtJ (NOD), and NZO/HlLtJ (NZO)) and three wild-derived strains (PWK/PhJ (PWK), CAST/EiJ (CAST), and WSB/EiJ (WSB)) [14]. These eight founder strains capture >90% of common genetic variation present in laboratory mouse strains and represent the three major subspecies of *Mus musculus* [15–17]. Importantly, this genetic variation exists across the genome, ensuring no blind spots for genetic mapping analyses. This genetic diversity has resulted in discovery of several genetic loci associated with a variety of biomedically relevant traits [18–24]. We and others have shown that there is extensive variation in splenic T cell populations [7], antibody glycosylation patterns [8], as well as variation in the general immune landscape of the spleen [10], across the CC population.

Here, we investigated how genetic variation impacts one aspect of systemic immune homeostasis: baseline serum antibody levels. We found that serum antibody levels for a variety of immunoglobulin (Ig) isotypes was highly varied across the CC, and we identified four quantitative trait loci (QTL) regulating these phenotypes. Three of the identified QTL mapped to known immunologically relevant regions of the genome, including the major histocompatibility locus and the immunoglobulin heavy chain locus. We also identified a novel locus broadly associated with variation in serum antibody levels, as well as B cell subset proportions in the spleen. Further analysis and independent mutant generation showed that the Methyl-CpG binding domain protein 1 (*Mbd1*) regulates homeostatic antibody levels and B cell differentiation, providing new insights into the genetic regulation of the humoral immune system and highlighting the utility of forward genetics-based discovery approaches in studying immunity.

Results

Variation in baseline antibody levels in the Collaborative Cross (CC) is largely driven by genetic factors

We quantified antibody concentrations in the serum of 117 mice from 58 CC strains (median = 3 mice/strain, 6–8 weeks old) to understand the role of genetic variation on homeostatic antibody levels. Serum from these mice was collected seven days after a non-specific footpad infection of phosphate buffered saline (PBS) with 1% fetal bovine serum (FBS), as these animals were control animals for another study. We assessed the concentrations of total IgA, IgM, and IgG, as well as IgG subtypes (IgG1, IgG2a, IgG2b, IgG2c, IgG3) in these sera by ELISA. We found that antibody concentrations varied greatly (3-50-fold) across these mice (**Fig 1 and S1 Table**). For example, IgM levels varied from 7.86 ug/mL– 271.39 ug/mL, total IgG levels ranged from 58.76 ug/mL– 173.89 mg/mL, and IgA varied from 4.39 ug/mL– 257.9 ug/mL in this population. Importantly, the variation between strains is much greater than that within strains (median standard deviation within strains is 0.596 ug/mL across all isotypes). We more formally assessed this by estimating the broad sense heritability (proportion of phenotypic variance in our population which can be attributable to genetic differences between individuals) for each of our antibody phenotypes and found that heritability estimates ranged from 0.25–0.66 (**Table 1**), indicating that genetic differences between strains plays a strong role in impacting this observed phenotypic variation in the CC. To understand the phenotypic relationships between antibody isotypes at homeostasis, we looked at pairwise correlations between all antibody isotypes and subtypes measured in the serum. We found that several antibody isotypes were highly correlated (mean correlation coefficient: 0.406, range: -0.115–0.841). We find that IgG1 levels were highly correlated with total IgG levels (correlation coefficient = 0.805), which was expected given the well characterized prevalence of IgG1 in the makeup of total IgG. However, we found additional interesting relationships among other antibody isotypes. For example, we found that IgA was highly correlated with both IgG2a (correlation coefficient = 0.645) and IgG2b (correlation coefficient = 0.543, **Fig 1**). These data suggest that there may be common genetic regulation of homeostatic antibody levels.

We next conducted genetic mapping to identify polymorphic genome regions associated with antibody level differences between the strains. QTL mapping identified four genome regions associated with variation in antibody levels (**Table 2**). *Qih1*, QTL for immune homeostasis 1 (Chromosome 18:73 – 78Mb, genome-wide $p < 0.2$), was identified for variation in homeostatic IgG1 levels, with the B6, CAST, and WSB haplotypes associated with higher levels of homeostatic IgG1. *Qih2* (Chromosome 17: 43.46–44.03Mb, genome-wide $p < 0.05$, **S1 Fig**) was identified for variation in homeostatic IgG2c levels, where NOD, B6, CAST, and NZO haplotypes were all associated with higher levels of IgG2c. Additionally for IgG2c, we

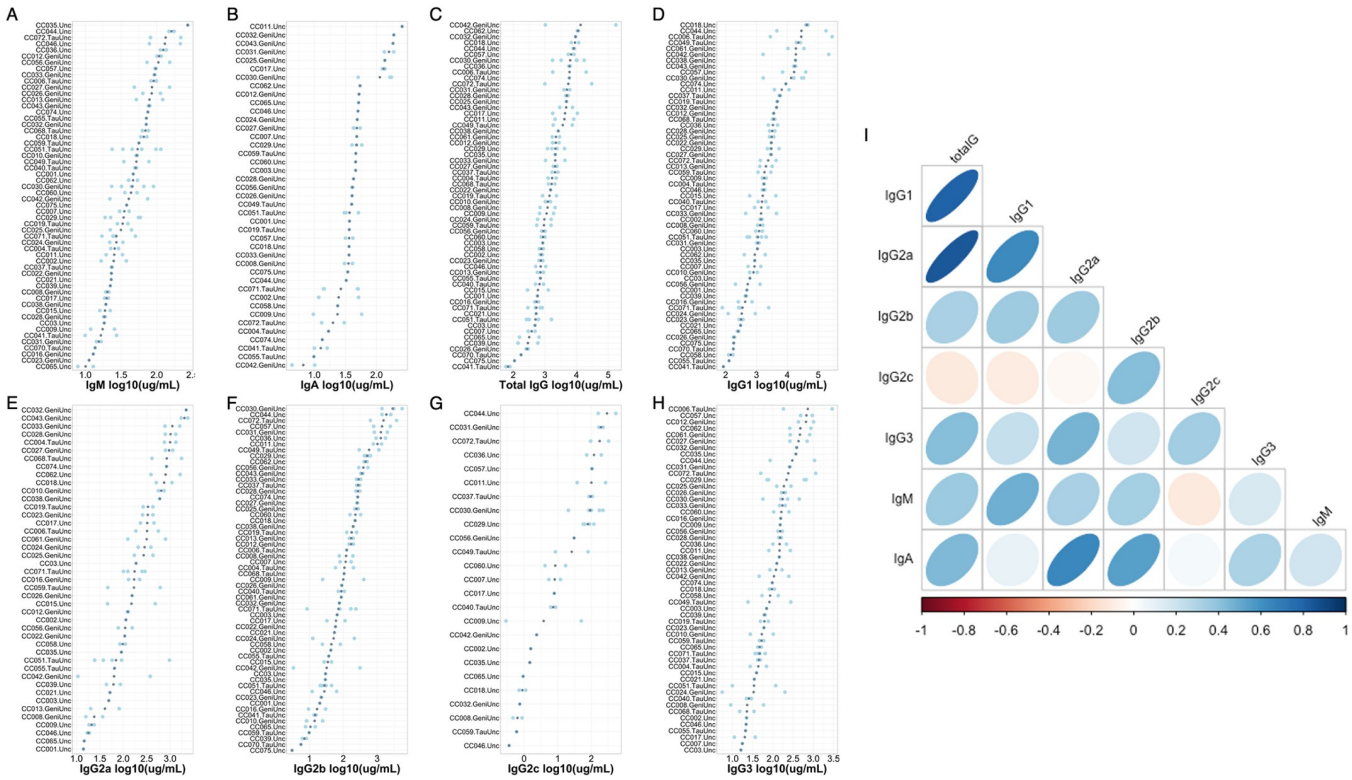

Fig 1. Variation in baseline antibody levels across CC strains and antibody isotypes. Total serum antibody levels for (A) IgM, (B) IgA, (C) total IgG, (D) IgG1, (E) IgG2a, (F) IgG2b, (G) IgG2c, and (H) IgG3 were quantified by ELISAs. Each plot is individually ordered so that the strain with the greatest strain mean is at the top of the plot and the strain with the lowest is at the bottom. Grey dots indicate the mean antibody concentration for an individual strain, and light blue dots indicate individual animal measurements. (I) the relationship between individual antibody isotypes and subtypes in the CC strains. Strains not included for a particular isotype (e.g. Panel B. IgA, Panel E. IgG2a, Panel G. IgG2c) had antibody levels that were undetectable for that isotype.

https://doi.org/10.1371/journal.pgen.1010548.g001

identified *Qih3* (Chromosome. 12:117.73–120.02Mb, genome-wide $p < 0.2$, S1 Fig), driven by the B6 and NOD haplotypes, which are associated with higher levels of IgG2c. Lastly, we found *Qih4* (Chromosome 12: 112.93–115.06Mb, genome-wide $p < 0.05$, S1 Fig) for variation in IgG2b levels at homeostasis. At this locus, B6 and NOD haplotypes are associated with higher levels of IgG2b. CAST, WSB, A/J, 129S1, and NOD haplotypes are intermediate, and the PWK haplotype is associated with lower levels of IgG2b.

It has long been suggested that expression of IgG2a and IgG2c is mutually exclusive in mouse strains based on the expression of IgG2a in BALB/c mice and IgG2c in B6 and SJL mice [25,26]. However, whether the genes controlling these isotypes were physically linked on the

Table 1. Homeostatic antibody serum concentration ranges and broad sense heritability estimates.

Antibody isotype	Phenotypic range (μg/mL)	Median phenotype value (μg/mL)	Broad sense heritability estimate
Total IgG	78.09–280910.17	1834.49	0.488
IgG1	58.76–173895.19	1498.06	0.518
IgG2a	10.71–2378.67	187.10	0.462
IgG2b	3.07–5448.50	149.16	0.641
IgG2c	0.29–536.33	79.45	0.661
IgG3	5.61–2906.31	101.02	0.249
IgM	7.87–271.39	44.22	0.561
IgA	4.39–257.93	41.63	0.375

https://doi.org/10.1371/journal.pgen.1010548.t001

Table 2. QTL identified in homeostatic antibody screen and causal haplotypes driving each QTL.

QTL Name	Antibody isotype	QTL interval	QTL threshold	Causal haplotypes
Qih1	IgG1	Chr. 18: 73-78Mb	$p < 0.2$	C57BL/6J, WSB/EiJ, CAST/EiJ—high
Qih2	IgG2c	Chr. 17: 43.4-44Mb	$p < 0.05$	C57BL/6J, NOD/ShiLtJ, CAST/EiJ, NZO/HlLtJ—high
Qih3		Chr. 12: 117.7–120.1Mb	$p < 0.2$	C57BL/6J, NOD/ShiLtJ–high
Qih4	IgG2b	Chr. 12: 112.9-115Mb	$p < 0.05$	C57BL/6J, NOD/ShiLtJ–high PWK/PhJ–low

https://doi.org/10.1371/journal.pgen.1010548.t002

same chromosome, or unique alleles at a locus was not understood. Recent work using isotype specific PCR showed that IgG2a and IgG2c were mutually exclusive in 4 inbred strains of mice: C57BL/6, NMRI, DBA2, and SJL, which the authors took as strong evidence of allelism [26]. Given that we mapped a QTL for IgG2c levels to the heavy chain locus (where the putative allelic variants of IgG2a and IgG2c exist), we examined these phenotypes and genotypes more closely and assessed the relationship between the CC founder haplotypes at this locus, sequence(s) unique to the IgG2a or IgG2c genes, and the CC strains abilities to produce either IgG2a (**S2A Fig**, IgG2a concentration (ug/mL)) or IgG2c (**S2B Fig**, IgG2c concentration (ug/mL)). Phenotypically (**Fig 2**), we found that CC strains with either the B6 or NOD haplotype at the *IgH* locus expressed IgG2c (> 0.00039 ug/mL, assay limit of detection) and did not express IgG2a, while strains with the other founder haplotypes at the locus expressed IgG2a (> 0.0039 ug/mL, assay limit of detection). While several of the samples containing the 129S1, A/J, NZO, CAST, PWK or WSB haplotypes at the locus were positive for IgG2c, these levels were quite low, and could be consistent with coincidental cross-reactivity of the detection antibodies used. To confirm this relationship more formally with previous analyses in the literature, we queried whole genome sequences of 24 CC strains [27,28] (3 strains with each of the founder haplotypes at *IgH*) using sequence strings that should exist as unique DNA sequences in the previously proposed IgG2c (CTCAAAGAGTGTCCCCCATGC)or IgG2a (AAGAACTGGGTGGAAAGAAATAGC) alleles [25,26]. We only found evidence for the sequence belonging to IgG2c in the genome sequences of CC strains containing B6 and NOD

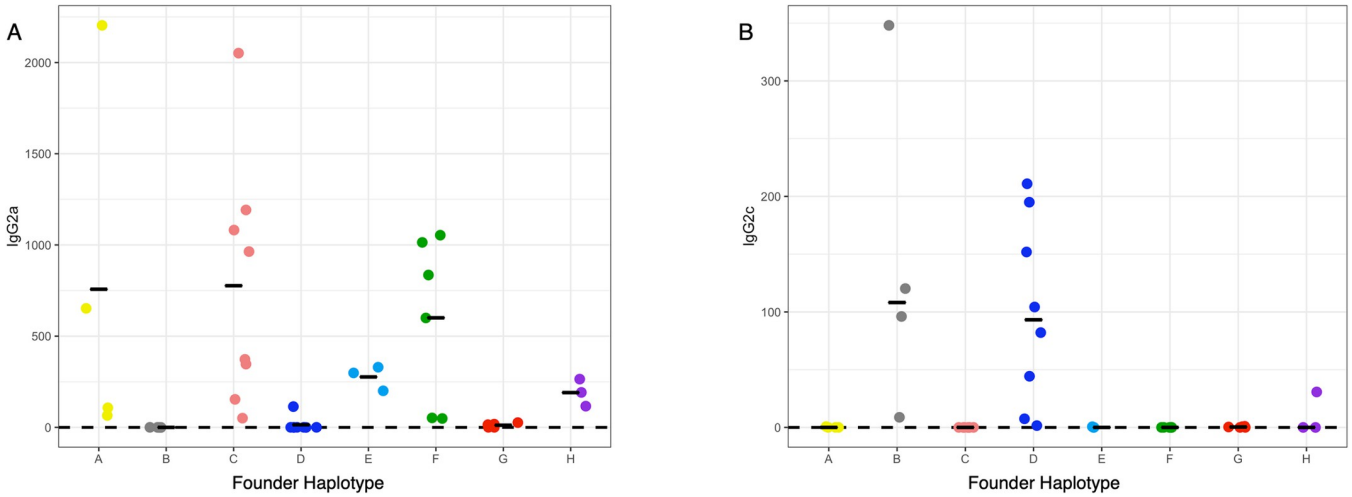

Fig 2. Expression of IgG2a and IgG2c by founder strain haplotype at the heavy chain locus. The mean value for IgG2a and IgG2c concentration (ug/mL) was determine for each CC strain. Mean values were plotted by the founder strain haplotype at the immunoglobulin heavy chain locus (Chromosome 12: 113 – 120Mb). Black bars indicate the mean concentration for a given founder haplotype and each individual point represents a strain with that founder haplotype at *Igh*. The y-axis is the concentration for IgG2a or IgG2c in ug/mL and the x-axis is the founder strain haplotype groups. Strains with undetectable concentrations of IgG2a or IgG2c were set to the lower limit of detection of the assay. Limit of detection represented by the dashed black line.

https://doi.org/10.1371/journal.pgen.1010548.g002

haplotypes (S2 Table) Similarly, CC strains with the 129S1, A/J, NZO, CAST, PWK and WSB haplotype at the locus only had sequence belonging to IgG2a, further reinforcing our intuition that the low levels of IgG2c detected in some of these strains represent spurious cross-reactivity. As such our data are consistent with, and strengthen the model proposed in [25,26] that IgG2a and IgG2c are, in fact, two alleles of the same gene. Concurrently, our ability to genetically map and associate these phenotypes to a prior implicated causal locus validates our larger genetic mapping approach.

Qih1 broadly impacts homeostatic antibody and splenic B cells

Given the proximity of *Qih2*, *Qih3*, and *Qih4* to known immunologically relevant genome regions *(Qih2* with the major histocompatibility complex (MHC), and *Qih3* and *4* with the immunoglobulin heavy chain (IgH) locus), we focused our attention on the novel *Qih1* (Fig 3). We first asked whether *Qih1* specifically regulated IgG1 levels (the initial trait for which we mapped the locus), or if it was more broadly associated with differences in the levels of other antibody classes and isotypes. We simplified the eight haplotype groups present in the CC into high- and low- response haplotypes at *Qih1* (BFH = high, ACDEG = low) using our previously established approach (Noll et al.). We found that there was a significant association between *Qih1* haplotype groups and total IgG (p = 1.627e-6, Fig 4B) and IgG2b (p = 0.0024, Fig 4E) levels, as well as marginal associations with IgG2a (p = 0.015, Fig 4D), IgG3 (p = 0.057, Fig 4G), and IgM (p = 0.068, Fig 4A) levels, suggesting that *Qih1* has broad effects on antibody levels at homeostasis.

We next addressed whether this genetic regulation of differences in antibody levels was due to intrinsic production differences of antibody on a per cell basis or could be due to the locus controlling the abundance of specific cell populations (e.g., B cells). We took advantage of an independent cohort of 89 mice from 48 CC strains (1–2 mice per strain, S3 Table) [29]. We analyzed splenocytes from these mice for high-level immune populations (e.g., T cells, B cells, dendritic cells, and macrophages) at homeostasis, as these mice had not had any specific immunological perturbations performed on them. As with our original antibody screen, we found that these cell populations were highly variable across animals (2-6-fold differences, S4 Table), and that most of this variation could be attributed to differences between genotypes (heritability of 0.24–0.76, S4 Table). As above, we again assigned these CC strains to either the high or low haplotype groups at *Qih1* and assessed the strength of relationships between these *Qih1* haplotypes and the measured cell populations. We found an association between *Qih1* and total $CD19^+$ B cells in the spleen (p = 0.041, Fig 5D), where CC strains with a high antibody level at Qih1 showed a decrease in the proportion of total splenic B cells. We also found marginal associations between *Qih1* and $CD3^+$ T cells (p = 0.088, Fig 5A) and $CD8^+$ T cells (p = 0.078, Fig 5C) in the same direction as the B cell relationship. However, we found no associations with $CD4^+$ T cells (p = 0.414, Fig 5B), $CD11b^+$ cells (p = 0.169, Fig 5E), or $CD11c^+$ cells (p = 0.612, Fig 5F) in this study. These results suggest that *Qih1* may broadly regulate multiple aspects of systemic immune homeostasis. However, consistent with its effects on antibody levels, the strongest relationship we observed was between *Qih1* haplotype and splenic B cell proportions.

Given the relationship between *Qih1* and both antibody levels and the relative abundance of total B cells within the spleen, we next assessed how *Qih1* impacts B cell development. We assessed total serum antibody levels and several B cell subsets in the spleen and bone marrow in 67 animals from a selected a set of 12 CC strains (2–8 mice/strain, 6 strains with a B6 haplotype, and 6 strains with contrasting NZO, NOD or PWK haplotypes at *Qih1*; S3 Table**).** We analyzed total $B220^+$ B cells, early, immature, and mature B cells in the bone marrow, as well as total $B220^+$, transitional, mature, and B1a ($CD5^+$) B cells in the spleen (S3 Table). Across

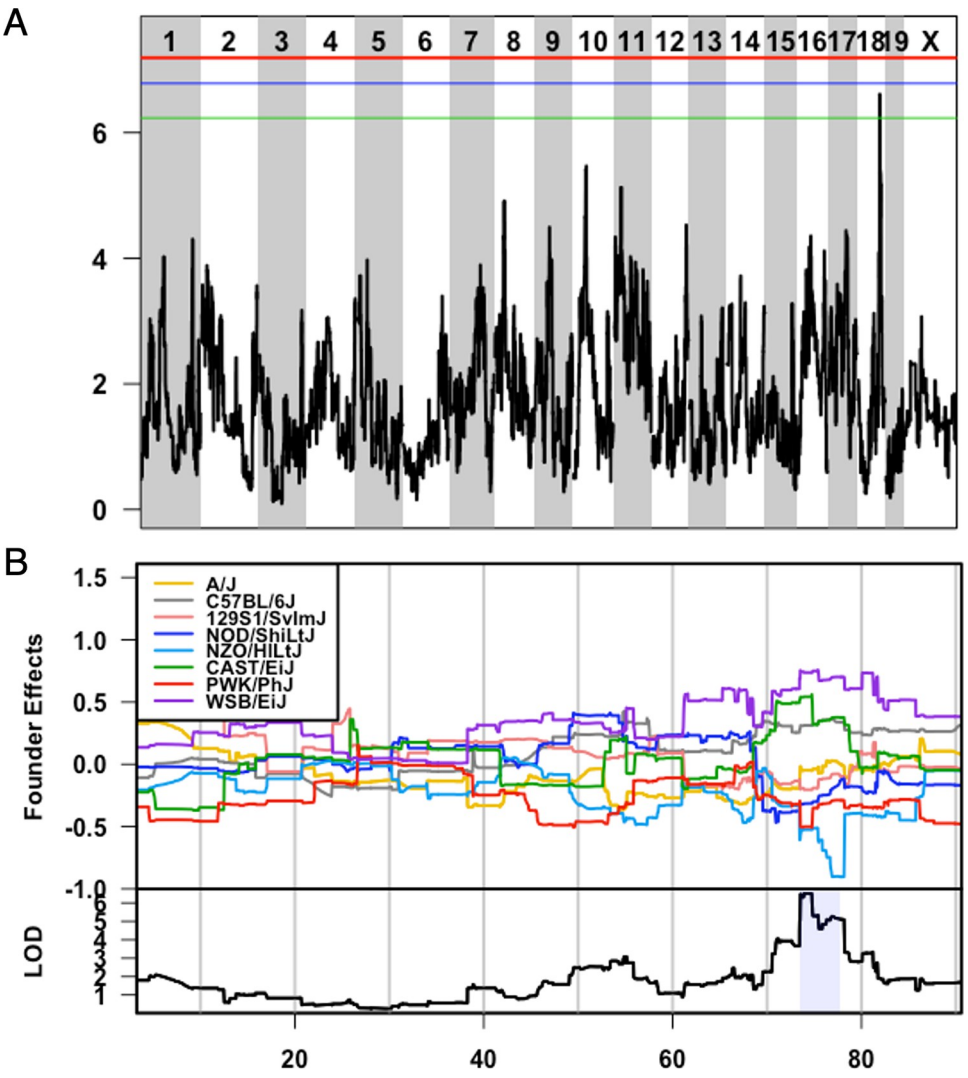

Fig 3. *Qih1* identified for variation in homeostatic IgG1 levels is driven by B6, WSB, and CAST haplotypes. A) LOD plot showing QTL significance (y-axis) across the genome (x-axis) with significance thresholds (genome-wide p-value = 0.05 (red), 0.1 (blue), 0.2 (green)). *Qih1* associated allele effects (A/J = yellow, B6 allele = grey, 129S1 allele = pink; NOD allele = dark blue; NZO allele = light blue; CAST = green; PWK = red; WSB = purple) were determined for the associated peak. B) Allele effect plot shows the mean deviation from population-wide mean as on the upper Y-axis for each allele segregating in the CC across the QTL peak region (x-axis positions are megabases on the chromosome) Highlighted region is the QTL confidence interval determined by a 1.5 LOD drop.

https://doi.org/10.1371/journal.pgen.1010548.g003

these B cell populations, we found that there was a trending association between splenic mature B cells and this locus (p = 0.102, S3C Fig), where animals with the B6 haplotype have lower levels. Concurrently, we validated that the B6 haplotype was associated with greater concentrations of both total IgG and IgG1 in the serum (S4 Fig). Taken together, these data suggest that *Qih1* may be regulating antibody levels in a B cell intrinsic manner.

MBD1 as a novel regulator of homeostatic antibody levels and splenic B cell subsets

Concurrent with our work investigating the immune mechanisms that *Qih1* causes variation in, we used our established QTL candidate analysis pipeline [23] to identify candidate genes

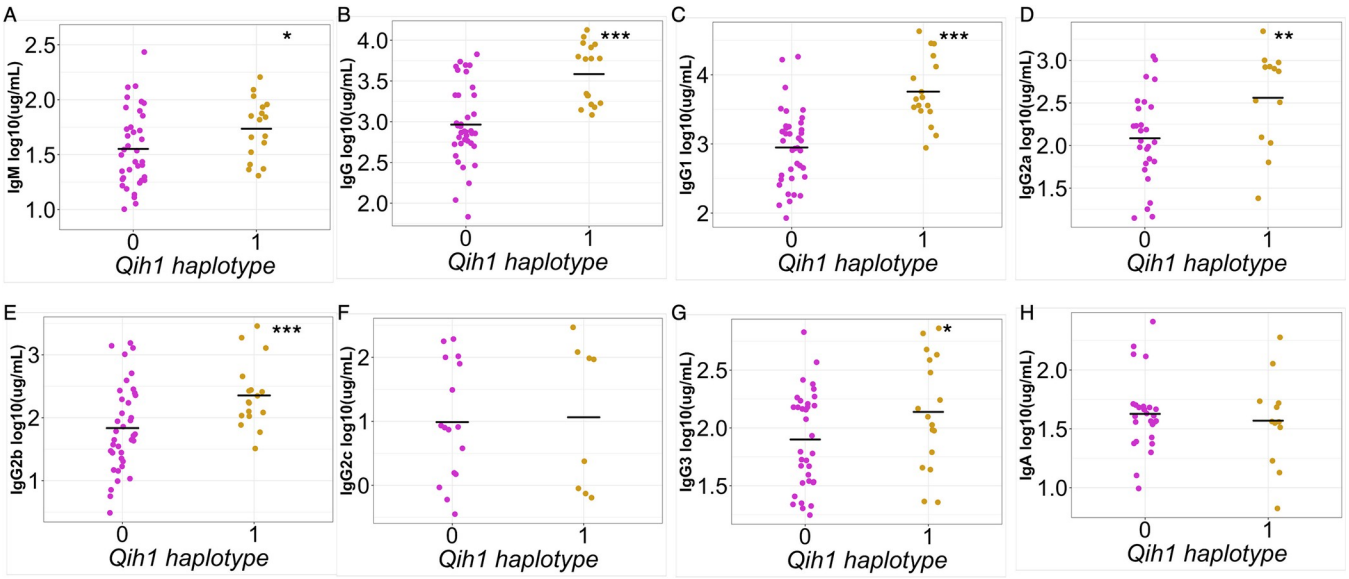

Fig 4. *Qih1* shows broad effects across antibody isotypes and subtypes. We assessed the relationship between B6, WSB, and CAST haplotypes (*Qih1* haplotype = 1) and serum concentrations of (A) IgM, (B) total IgG, (C) IgG1, (D) IgG2a, (E) IgG2b, (F) IgG2c, (G) IgG3, and (H) IgA. Each point represents the mean value for each CC strain and the mean for each haplotype group on the x-axis is denoted by the grey crossbar. ($^{*}p < 0.1$, $^{**}p < 0.05$, $^{***}p < 0.01$) p-values determined using nested linear model approach described in the methods.

https://doi.org/10.1371/journal.pgen.1010548.g004

underlying the effects of *Qih1*. Briefly, we first filtered all genes under the locus down to genes expressed in the spleen. Then, we further filtered this gene set down to genes with genetic variants that fit with the allele effects of *Qih1*. Within the *Qih1* locus, there are only 14 protein coding genes, and 10 of these genes had variants specific to the 3 causal haplotypes (in total 12 genes with CAST-private variants, 11 genes with WSB-private variants, and 11 genes with B6-private genetic variants). However, while there were no common variants across all three haplogroups, one gene, *Mbd1*, contained missense or nonsense (protein sequence) variants that were specific to each of the causal haplotypes (six genes contained CAST-private protein effecting variants, WSB- and B6-private protein effecting variants only occurred in this one gene). As such, we focused our downstream analysis on the role of Methyl-CpG binding domain protein 1 (*Mbd1*) in regulating baseline antibody and B cell variation.

As noted above, there were no common missense variants in *Mbd1* segregating B6, CAST and WSB from the other founder strains. However, all three strains possessed independent missense variants (WSB: rs36715598, SIFT: 0.05; CAST: rs36834535, SIFT: 0.24 and rs222802617, SIFT: 0.09; and B6: rs46321411, SIFT: 1, rs46176119, SIFT: 0, and rs30250376, SIFT: 1). Of note was the excess of non-synonymous differences between B6 and the other common laboratory strain founders of the CC. Therefore, we further investigated the amino acid sequence variation among 29 additional mouse strains and 3 additional species (rats, non-human primates, and humans) (**S3 Table**). [30,31] Besides the other Clarence Little strains (C57BL/6NJ, C57BL/10J, C57BR/cdJ, C57L/J, C58/J), only ST/bJ, BUB/BnJ (2 variants) and the wild derived ZALENDE/EiJ strains had these 'B6' variants. Given the otherwise high level of amino acid conservation in MBD1 across mouse strains, rats, non-human primates, and humans, this indicates that the B6 allele of *Mbd1* is both highly evolutionarily derived in this region and likely of a single wild origin that was only introduced into a subset of mouse inbred strains.

MBD1 has been previously shown to be involved in T cell development (consistent with our above observation that there were T cell differences in some of our CC analyses) and

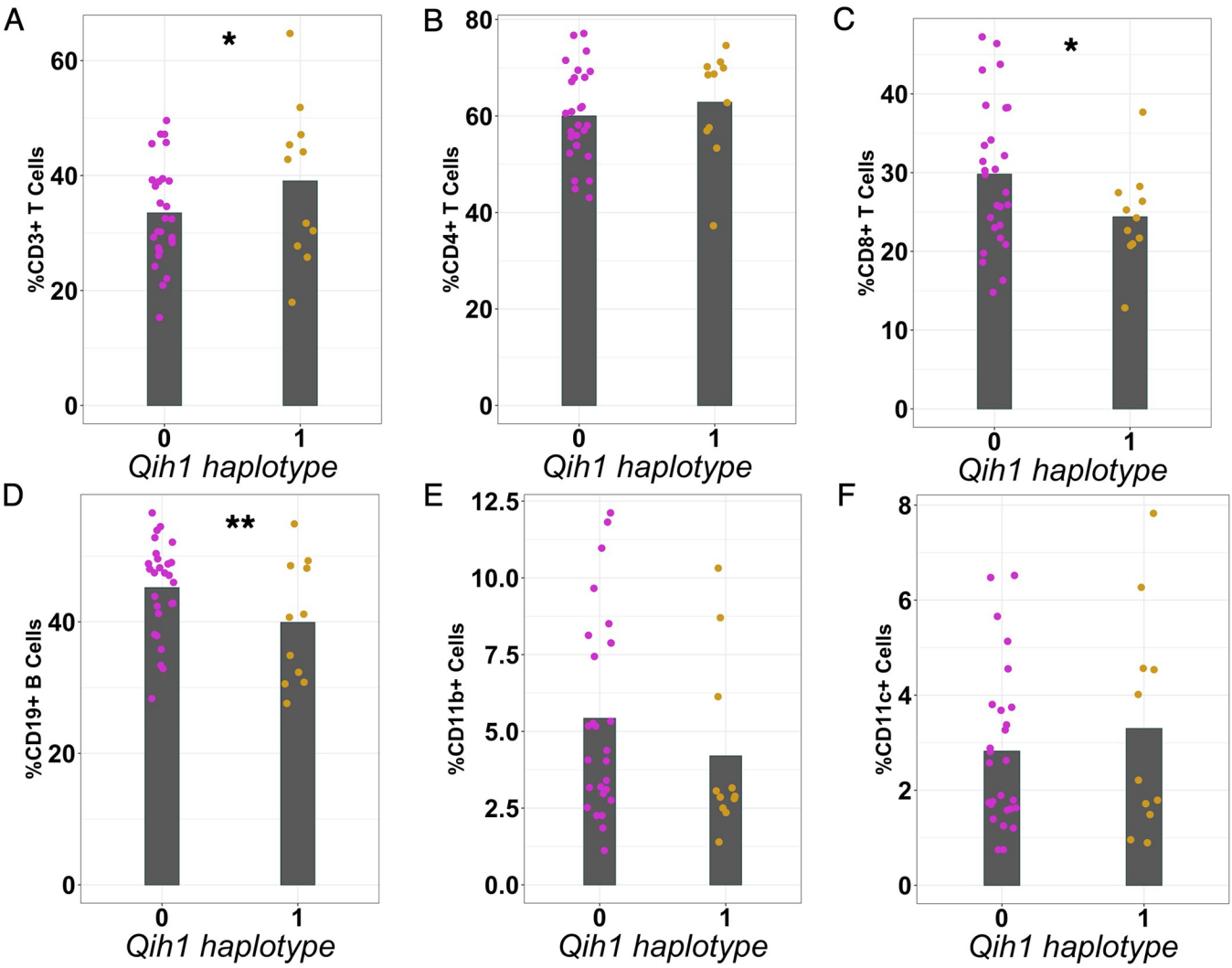

Fig 5. *Qih1* shows broad effects on immune cell populations in the spleen. We assessed the relationship between B6, WSB, and CAST haplotypes (*Qih1* haplotype = 1) and (A) $CD3^+$ T cells, (B) $CD4^+$ T cells, (C) $CD8^+$ T cells, (D) $CD19^+$ B cells, (E) $CD11b^+$ cells, and (F) $CD11c^+$ cells in the spleen. Each point represents the mean value for each CC strain and the mean for each haplotype group on the x-axis is denoted by the grey crossbar. ($^*p < 0.1$, $^{**}p < 0.05$) p-values determined using nested linear model approach described in the methods.

https://doi.org/10.1371/journal.pgen.1010548.g005

autoimmunity [32], neural development [33,34], and adipocyte differentiation [35]. While *Mbd1* deficient animals have been previously generated, these mice were initially generated on the 129S4 genetic background [36], and then backcrossed to C57BL/6. Given that 129 (129S1 in the case of the CC) and C57BL/6 had opposing haplotype effects, this makes it difficult to differentiate whether effects on baseline antibody or B cell populations are due to the lack of *Mbd1*, or other variants in the locus. Therefore, we generated a new *Mbd1* knockout (KO) directly on the C57BL/6J genetic background by CRISPR gene editing to directly test whether MBD1 specifically plays a role in regulating homeostatic antibody levels and more broadly, B cell subset differences.

Using a heterozygote-x-heterozygote breeding design, we found that early adult (6-8wk old) *Mbd1* KO animals had several antibody and B cell related differences relative to their WT littermates. Specifically, mutant mice had lower levels of IgG1 in the serum compared to WT littermates (**Fig 6**, recapitulating our observations in the CC). They also had significant

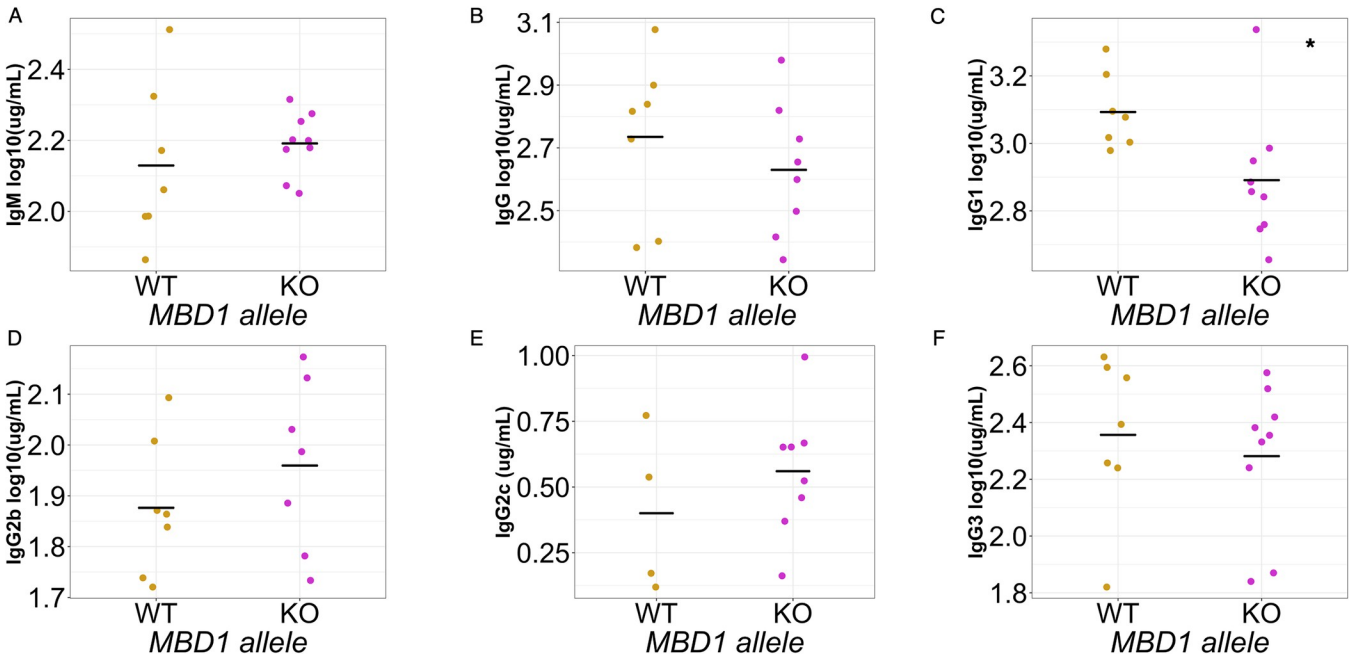

Fig 6. MBD1 regulates homeostatic serum IgG1 levels. Log10 transformed serum antibody concentrations for (A) IgM, (B) total IgG, (C) IgG1, (D) IgG2b, (E) IgG2c, and (F) IgG3. The data shown represent one of two independent experiments, each performed with 6–9 animals from each genotype. Each point represents an individual animal measurement, and the grey crossbar indicates the mean for each genotype. (*$p < 0.05$) p-values determined using Student's t test.

https://doi.org/10.1371/journal.pgen.1010548.g006

increases in marginal zone B cell numbers and proportions (of all B cells) in the spleen, with no differences in total, transitional, or follicular B cells (Fig 7). Given that marginal zone B cells can rapidly differentiate into antibody secreting cells and the inverse relationship between MZBs and antibody levels in our KO mouse, we measured $CD138^{+}$ antibody secreting cells in the spleen. As expected, we found a decrease in antibody secreting cell abundances in the spleens of *Mbd1* KO animals, corresponding to the decrease in antibody and increase in MZBs (**Figs 7E, 7J and S5**).

In a separate cohort of animals, we aged them further to maturity (15–16 weeks old), and assessed IgG1, total IgG and IgM levels. We found that *Mbd1* KO animals maintained reduced levels of antibodies (total IgG and IgM, **S2 Fig**) relative to their wild type littermates through this age. All told, our data in this *Mbd1* KO stock are consistent with the haplotype effects on baseline antibody and B cell populations observed in the CC, indicate that MBD1 is a negative regulator of marginal zone B cell differentiation and a suppressor of antibody secretion. Thus, it is likely that MBD1 acts to regulate marginal zone B cell differentiation into an antibody secreting cell, and genetic polymorphisms in the *Mbd1* gene contributing to variation in baseline antibody levels and B cell proportions are due to a potential role in this differentiation process.

Discussion

Immune homeostasis is the state in which the immune system is maintained in the absence of specific insults. This balanced state is critical in ensuring an efficient response when challenged, while concurrently limiting immune pathology or unwanted (e.g. allergic) responses. The immune homeostatic state varies greatly in humans [3–4, 11–12] and has been shown to influence responses to immunotherapies and vaccination [1,3]. Therefore, understanding the genetic mechanisms that regulate the homeostatic state is critical to understanding an

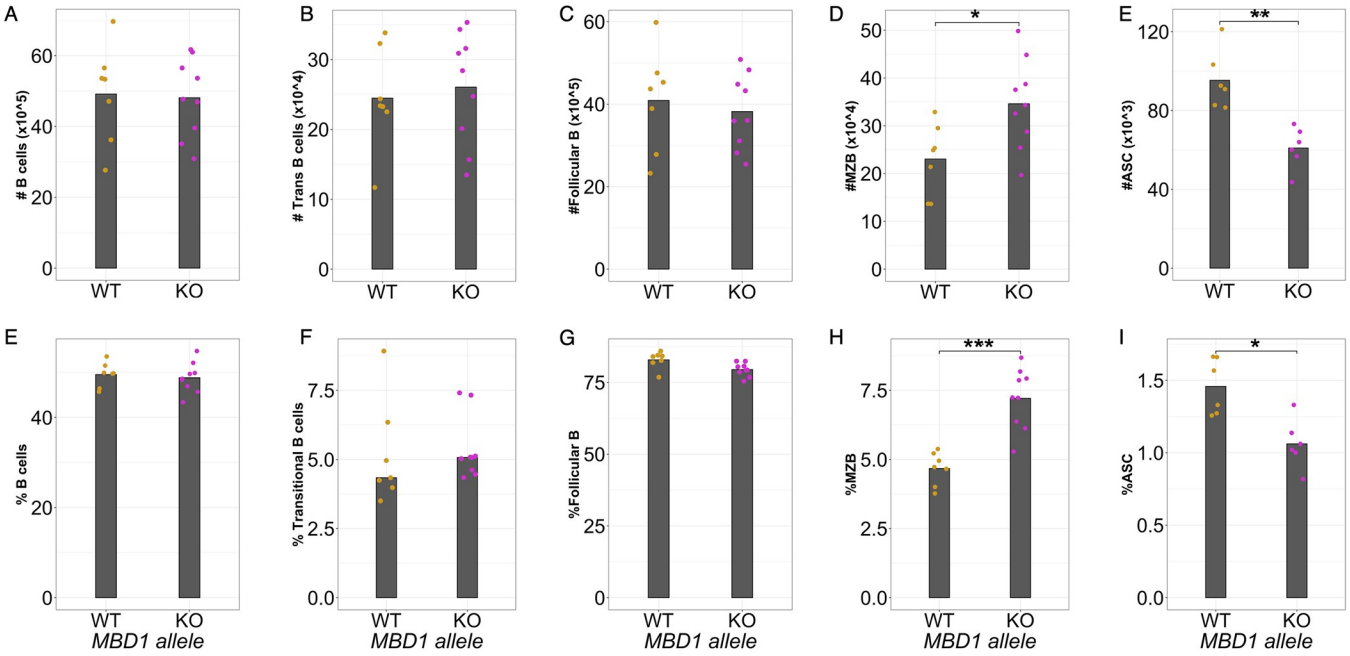

Fig 7. MBD1 regulates B cell subsets at homeostasis. The number and proportion of (A, E) CD19+, B220+ B cells, (B, F) transitional B cells, (C, G) follicular B cells, (D, H) marginal zone B cells, and (E, I) antibody secreting cells were measured in the spleen at baseline The data shown represent one of two independent experiments, each performed with 6–9 animals from each genotype. Each point represents an individual animal measurement, and the grey crossbar indicates the mean for each genotype. ($^{*}p < 0.05$, $^{**}p < 0.01$, $^{***}p < 0.001$) p-values determined using a Wilcoxon Ranked Sum test.

https://doi.org/10.1371/journal.pgen.1010548.g007

individual's potential to respond to pathogen challenge. However, it is challenging to study immune homeostasis in human populations due to environmental factors like prior pathogen exposure, diet [37], or environmental insults [38]–all of which concurrently can perturb the immune system, As such, mouse models have been critical for identifying and understanding genes that regulate immune development and homeostasis [39–43]. We extend this body work by describing variation in homeostatic antibody levels across the Collaborative Cross population and identify four QTL that are associated with variation in three different IgG subtypes (IgG1, IgG2b, IgG2c).

Three of these QTL map to known immunologically important regions, *Qih2* (mapped for IgG2c) is located near the major histocompatibility locus, and *Qih3* (mapped for IgG2c) and *Qih4* (mapped for IgG2b) are located at or near the immunoglobulin heavy chain locus. Both loci have long and well characterized associations with immune responses. Specifically, the MHC locus is overrepresented in genes involved in processing and presentation of foreign peptides to generate adaptive responses. Similarly, the Ig heavy chain locus contains genes necessary for generating the heavy chain component of every antibody isotype. Both regions are gene dense, have copy number variation, as well as gene family birth and loss [30]. As such, it was challenging for us to narrow these down to specific candidates for these loci, however our results point to the highly variable nature of the immune responses across the CC. We also identified a novel locus, *Qih1*, associated with variation in IgG1 levels at homeostasis, and demonstrated that this locus had broader effects on total antibody levels and splenic immune cell populations. Lastly, we identified a gene underneath *Qih1*, *Mbd1*, as a novel regulator of homeostatic antibody and marginal zone B cell differentiation to antibody secreting cells.

Our initial study focused on a variety of circulating antibody isotypes, and we identified loci at or near the major histocompatibility (MHC) locus and the immunoglobulin heavy chain (IgH) locus that are associated with variation in IgG2a/c or IgG2b. These loci validate

our approach, as they serve as strong positive controls for regions known to be important for antibody levels. However, they can also inform potential mechanisms driving differences in total homeostatic antibody levels. *Qih4* (mapped for IgG2b), located near the IgH locus, would potentially suggest cis-regulatory elements which control expression or regulation of IgG2b alleles. *Qih2* (mapped for IgG2c), located near MHC, may indicate a haplotype specific manner of antigen detection and presentation that influences IgG2c expression or relate to the regulation of adaptive immune cell crosstalk, more generally. However, defining the specific mechanism by which *Qih2* regulates IgG2c levels requires additional analysis of T cell responses and potentially other aspects of innate immune crosstalk with the adaptive B cell compartment. More broadly, various antibody isotypes and subtypes are important for different aspects of the immune response [44,45]. In our study, we have identified divergent haplotypes across loci regulating antibody levels at homeostasis, which suggests that independent genetic regulation arose from antigenic exposure histories in the evolution of various mouse strains [46].

Our mapping allowed us to return to an observation long known in the literature: that laboratory mice tend to produce either IgG2a or IgG2c, but not both [25]. Additionally, even in outbred mice it was somewhat unclear if these represented two alleles or paralogues closely linked on the same chromosome [25,26]. As described above, we found that CC strains with either B6 or NOD haplotypes at the IgH locus expressed IgG2c and strains with the other founder haplotypes at the locus expressed IgG2a. Concurrently, we took advantage of whole genome sequence data of the CC strains. We identified probe sequences from the original characterization of the IgG2a and IgG2c paralogues and confirmed for strains with a B6 or NOD haplotype at IgH that they not only expressed IgG2c, but that there were only genome sequence reads for the IgG2c gene. Likewise, strains with either A/J, 129S1, NZO, CAST, WSB, or PWK haplotypes at IgH only contained genome sequence reads for the IgG2a gene and not IgG2c. These data indicate that IgG2a and IgG2c indeed represent two distinct alleles in the mouse genome. It has been noted that there are functional differences between IgG2a and IgG2c [47], and these results can help investigators identify relevant mouse strains with specific IgG2 subtypes for functional follow-up to these two alleles.

B cells play a critical role in immune system development and homeostasis. Specific subsets of B cells, B1 and marginal zone B cells, differentiate to antibody secreting cells to produce natural antibodies, which are present before antigen stimulation and provide a first line of defense against infection [48–51]. Natural antibodies are characterized by their broad reactivity and low affinity and are pre-existing or immediately secreted upon stimulation or a 'light push' [48]. These antibodies are largely thought to bridge the gap between innate and adaptive immunity and have been studied for their ability to protect against various pathogens [51,52]. Several aspects of natural antibody have been investigated, but it is still largely unclear how these antibodies are regulated and under what contexts they are produced [48,53]. Here we identify a novel genetic regulator, *Mbd1*, of pre-existing antibody, marginal zone B cell, and antibody secreting cell levels at homeostasis. Our data suggests that MBD1 inhibits marginal zone B cell differentiation to antibody secreting cells at homeostasis, thus regulating pre-existing antibody levels.

MBD1 is a known epigenetic regulator, facilitating chromatin remodeling through various protein-protein interactions, binding directly to methylated DNA, and facilitating transcriptional repression [54,55]. Much of what is known about MBD1's function comes from studies of neural stem cell differentiation [33] and adipocyte differentiation [35]. In the immune system, previous work has shown that MBD1 facilitates tissue-specific antigen expression through protein-protein interactions with AIRE to promote T cell tolerance [32]. However, MBD1 has not been described as having a role in B cell differentiation. Chromatin modifying complexes and other epigenetic regulators are critical to cellular differentiation, as chromatin accessibility changes over differentiation states allows for proper gene expression. Recent work has highlighted

the important role of epigenetic regulators in B cell activation and differentiation. For example, EZH2 [56], LSD1 [57], and DNA methylation [58,59] have all been shown to regulate some aspect antibody secreting cell differentiation. While we do not provide a direct link between MBD1 function and antibody secreting cell differentiation, our data suggests it is likely that MBD1 is regulating chromatin dynamics necessary for altering gene expression profiles that promote antibody secreting cell differentiation. Thus, understanding the role of MBD1 in regulating gene expression profiles necessary for B cell differentiation will be important for defining those genes and regulatory networks that control B cell responses at homeostasis, as well as following infection and activation of adaptive immune responses. serving a comparable role.

Our study encompasses experiments using several cohorts of CC strains with varying ages and experimental designs, as well as a new *Mbd1* knockout model on the B6 background. While we find that the B6 allele is consistently associated with greater antibody levels and lower splenic B cell proportions in the CC, we were not able to recapitulate all those phenotypes in our knockout studies. For example, in the CC the B6 haplotype is not only associated with greater levels of IgG1 in the serum but also greater levels of total IgG and marginally associated with greater levels of other antibody subtypes. However, we were only able to recapitulate the impact of MBD1 on IgG1 levels, specifically, in the context of our knockout model. It is not entirely surprising that we are not able to completely recapitulate every phenotype observed in the larger initial screen. In the CC, allelic variants across many genetic backgrounds are averaged, while a knockout represents an extreme abrogation in the context of a single genetic background. In inbred B6 mice, the evolutionarily derived allele of *Mbd1* has co-evolved with protein binding partners and regulatory networks, whereas in the CC, those co-evolved networks have been broken apart and alleles are shuffled out of context. Additionally, there are 2 other founder strain haplotypes that were associated with greater antibody levels in the CC, and we do not capture their contributions in our knockout studies. Lastly, we do not map 100% of the genetic regulators of IgG1, as *Qih1* only accounts for ~75% of the genetic regulation of IgG1 levels at homeostasis. Although, *Qih1/Mbd1* has a large effect, there are other genes that contribute to the regulation of IgG1 and marginal zone B cell differentiation at homeostasis. None the less, we find a consistent role for *Qih1/Mbd1* on homeostatic antibody levels and various B cell subsets across our experimental populations. Specifically, we found that a functional B6 *Mbd1* allele is consistently associated with greater levels of homeostatic antibody and lower levels of various B cell subsets in the spleen. Interestingly, the association between the B6 allele and lower levels of B cell subsets was not observed in the bone marrow (**S3 Fig**), suggesting that overall B cell development was intact.

In summary our data provide evidence for strong genetic regulation of homeostatic immunity. We also show the utility of forward genetic screens in diverse mouse populations for identifying novel genes regulating homeostatic immunity. To our knowledge this is the first demonstration that MBD1 may act as a negative regulator of marginal zone B cell differentiation to antibody secreting cells, thereby regulating antibody levels at homeostasis. Additionally, our data further illustrates the role of epigenetic regulators in cellular differentiation and function. Future work to elucidate the specific pathways controlled by MBD1 to regulate marginal zone B cell differentiation could enhance our understanding of marginal zone B cell mediated humoral immunity at homeostasis and in response to pathogen infection.

Methods

Ethics statement

All mouse experiments were conducted under protocols approved by the University of North Carolina at Chapel Hill's Institutional Animal Care and Use committee, which is AAALAC accredited.

Mice

Collaborative Cross mice. CC mice were obtained from the UNC Systems Genetics Core Facility at the University of North Carolina at Chapel Hill between 2013–2017. All experiments were approved by the University of North Carolina at Chapel Hill Institutional Animal Care and Use Committee. Mice were sacrificed using isoflurane overdose and terminally bled by cardiac puncture at six to twelve weeks of age depending on the experiment. For the initial baseline antibody screen, experiments were conducted under biosafety level 3 (BSL3) conditions where four to six weeks old female mice were cohoused across strains and allowed to acclimate to the BSL3 for 3–4 days. Mice were then inoculated subcutaneously in the left rear footpad with phosphate-buffered saline (PBS) supplemented with 1% fetal bovine serum (FBS). All other CC studies were conducted in standard animal housing facilities.

Mbd1 knockout mouse

Mbd1 knockout mice were generated at the University of North Carolina at Chapel Hill by the Animal Models Core via CRISPR mutagenesis. Specifically, Cas9 guide RNAs were designed with Benchling software and used to generate a 752bp deletion spanning exons 11 and 13, which resulted in protein ablation. The presence of the knockout or wildtype allele was determined by amplifying across the region using the following primers: forward primer–GCTCACTGAGTAGGGCAAGG, reverse primer–TACGGAGCACACCTTGGCA. Wildtype amplicon: 1262bp. Knockout amplicon: 510bp. We maintained these mice in our colony via 2 generations of backcrossing to C57BL/6J mice (JAX stock #000664) to remove any potential off-target mutations. The stock was thereafter maintained via het-by-het crosses.

ELISA

Total antibody levels were quantified by ELISA. 96-well flat-bottom high-binding plates were coated with anti-Ig antibodies (Southern Biotech) diluted in carbonate buffer for each antibody subtype measured. Serum was diluted in ELISA wash buffer (1x PBS + 0.3% Tween20) with 5% nonfat milk and added to pre-coated plates to incubate in humid storage overnight at 4˚C. Plates were washed using ELISA wash buffer and incubated with HRP-conjugated anti-Ig secondary antibodies (Southern Biotech) for 2 hours in humid storage at 4˚C. Plates were washed and developed in the dark for 30 minutes at room temperature with citrate substrate buffer, the reaction was stopped with sodium fluoride, and read immediately at 450nm. Standard curves for each antibody subtype (Invitrogen standards) were run with each plate for a specific subtype to determine antibody concentrations.

Sample preparation

Following euthanasia (as described above), blood was collected immediately into serum separator tubes to isolate serum for ELISAs. Serum was aliquoted in 1.7mL Eppendorf snap-cap tubes and stored at -80˚C until analyzed by ELISA. Spleens were homogenized using frosted microscope slides and pelleted by centrifugation (1000 RPM/4˚C/10 minutes). Spleen homogenates were filtered through 70um mesh, treated with ammonium chloride potassium (ACK) lysing buffer to remove red blood cells, washed, and resuspended in FACS buffer (HBSS + 1–2% FBS). Cell numbers were determined by trypan blue exclusion using a hemocytometer or Countess II automated cell counter.

Flow cytometry

Cells were plated at 1-2x10^7 per mL in FACS buffer (HBSS + 1–2% FBS) in a 96-well polypropylene round-bottom plate. Cells were centrifuged at 1000 RPM for 4 minutes at 4˚C and resuspended in 100uL of fluorochrome-conjugated antibody dilution. Cells were incubated at 4˚C for 45 minutes to allow for antibody staining. Following incubation, cells were washed twice with FACS buffer and resuspended in 100uL of FACS buffer. An equal volume of 4% PFA (in PBS) was added to cells to fix, and plates were stored in the dark at 4˚C until analyzed of Attune NxT flow cytometer. Data was analyzed using FlowJo software. The following antibodies were used: Live/Dead Fixable Aqua, CD3-PE (145-2C11), CD4-APC/Cy7 (GK1.5), CD8a-PerCP(53–6.7), CD11b-eF450 (M1/70), CD11c-PE/TxRd (N418), CD19-AF647 (6D5), CD45-AF700 (30-F11), CD19-APC/Cy7 (6D5), IgM-PE (ll/41), IgD-FITC(11-26c.2a), CD5-BV421 (53–7.3), CD3-PerCP (145-2C11), CD21/CD35-PE (7E9), IgM-AF594, CD23-PE/Cy7 (B3B4), CD45R-APC (RA3-6B2).

Data processing

Antibody concentrations were determined from a standard curve and $\log_{10}$ transformed to follow a normal distribution. Event counts from flow cytometry gating were used to calculate cell proportions. Using Box-Cox transformation (MASS package in R, version 3.5.1), values were independently transformed for each phenotype to follow a normal distribution. For all phenotypes used for QTL mapping, the average phenotype value was calculated for each Collaborative Cross strain and used to map.

Statistical analysis

Nested linear models. Correlations between identified QTL and immune cell populations and other antibody subtypes were determine by comparing the goodness of model fit of mixed effect linear models using a partial fit F-test. *Qih1* haplotype scores were determined by the founder haplotype at the *Qih1* peak marker. In both the base and full model, CC Strain is a random effect variable and *Qih1* haplotype score is a fixed effect variable. The full model tests whether including information about the haplotype at *Qih1* explains more of the phenotypic variation than the CC Strain alone.

Base model: Phenotype ~ CC Strain + error

Full model: Phenotype ~ CC Strain + *Qih1* haplotype score + error

Statistical significance for phenotypes compared between wild-type and *Mbd1* knockout mice was determined using a Wilcoxon Ranked Sum test.

Broad sense heritability estimates

Heritability calculations were performed as described previously (Noll et al., 2020). Briefly, box-cox transformed phenotype values were used to fit a linear fixed-effect model. The coefficient of genetic determination was calculated as such:

$$(\mathbf{MS_{CC-F1}} - \mathbf{MS\varepsilon})/(\mathbf{MS_{CC-F1}} + (\mathbf{2N-1})\mathbf{MS\varepsilon})$$

Where $MS_{CC\text{-}F1}$ is the mean square of the CC-F1 and MSε is the mean square of the error using a N = 3 as an average group size, as a measure of broad-sense heritability.

QTL mapping

QTL mapping was performed as previously described [23,24]. Briefly, we used the DOQTL [60] package in the R statistical environment (version 3.5.1). A multiple regression is

performed at each marker, assessing the relationship between the phenotype and the haplotype probabilities for each strain. LOD scores are calculated based on the increase in statistical fit compared to a null model, considering only covariates and kinship. To calculate significance thresholds, permutation tests were used to shuffle genotypes and phenotypes without replacement. We determined the 80^{th}, 90^{th}, and 95^{th} percentiles after 500 permutations as cutoffs for suggestive (both $p<0.2$ and $p<0.1$) and genome-wide significant ($p<0.05$). QTL intervals were determined using a 1.5 LOD drop.

Supporting information

S1 Fig. QTL scans and haplotype effect plots for IgG2b and IgG2c phenotypes depicting *Qih2*, *Qih3*, and *Qih4*.
(TIFF)

S2 Fig. *Mbd1* KO mice have lower levels of antibody with increased age. We assessed IgG1, Total IgG, and IgM levels in the serum of 15-16wk old animals. Each point represents an individual animal and the median for each genotype group on the x-axis is denoted by a crossbar. ($^{*}p < 0.05$)
(TIFF)

S3 Fig. *Qih1* effects on B cell populations in the spleen and bone marrow. We assessed the relationship between B6, WSB, and CAST haplotypes (*Qih1* haplotype = 1) and spleen total $B220^{+}$ B cells (A), transitional (IgM^{var}, IgD^{-}) B cells (B), mature (IgM^{var}, IgD^{+}) B cells (C), B1 ($CD5^{+}$) B cells (D), and bone marrow total $B220^{+}$ B cells (E), early (IgM^{-}, IgD^{-})B cells (F), and immature (IgM^{+}, IgD^{-}) B cells (G). Each point represents the mean value for each CC strain and the mean for each haplotype group on the x-axis is denoted by the grey crossbar. ($^{\#}p < 0.2$, $^{*}p < 0.1$)
(TIFF)

S4 Fig. Validation of the impact of *Qih1* on baseline IgG1 and total IgG levels in the serum. We assessed the relationship between B6, WSB, and CAST haplotypes (*Qih1* haplotype = 1) and serum total igG and IgG1 levels. Each point represents the mean value for each CC strain and the mean for each haplotype group on the x-axis is denoted by the grey crossbar.
(TIFF)

S5 Fig. B cell gating scheme for Fig 7.
(TIFF)

S1 Table. p-values for antibody concentration correlations presented in Fig 1. P-values were determined using the cor.test function in R stats package (version 3.5.1).
(DOCX)

S2 Table. Sequence evidence for alternative alleles for IgG2a and IgG2c.
(DOCX)

S3 Table. CC and inbred mouse strains used in these studies.
(DOCX)

S4 Table. Phenotype distribution and heritability of 48CC screen phenotypes.
(DOCX)

S5 Table. Narrow sense heritability estimates for baseline serum antibody concentrations presented in Fig 1 and Table 1.
(DOCX)

Acknowledgments

We wish to thank the Systems Genetics Core Facility for the maintenance of the Collaborative Cross lines used in these studies. We would also like to thank the UNC Flow Cytometry Core for their help with flow cytometry data acquisition and analysis.

Author Contributions

Conceptualization: Brea K. Hampton, Kenneth S. Plante, Alan C. Whitmore, Martin T. Ferris, Mark T. Heise.

Data curation: Brea K. Hampton, Kenneth S. Plante, Alan C. Whitmore, Colton L. Linnertz, Emily A. Madden, Kelsey E. Noll, Samuel P. Boyson.

Formal analysis: Brea K. Hampton, Kenneth S. Plante, Alan C. Whitmore, Colton L. Linnertz, James G. Xenakis.

Funding acquisition: Fernando Pardo-Manuel de Villena, Martin T. Ferris, Mark T. Heise.

Investigation: Brea K. Hampton, Kenneth S. Plante, Alan C. Whitmore, Emily A. Madden, Kelsey E. Noll, Samuel P. Boyson, Breantie Parotti, Timothy A. Bell, Pablo Hock, Ginger D. Shaw.

Methodology: Brea K. Hampton, Kenneth S. Plante, Emily A. Madden, Kelsey E. Noll, Samuel P. Boyson, Breantie Parotti, Timothy A. Bell, Pablo Hock, Ginger D. Shaw.

Resources: Mark T. Heise.

Supervision: Martin T. Ferris, Mark T. Heise.

Validation: Brea K. Hampton, Alan C. Whitmore, Mark T. Heise.

Visualization: Brea K. Hampton.

Writing – original draft: Brea K. Hampton, Martin T. Ferris, Mark T. Heise.

Writing – review & editing: Brea K. Hampton, Kenneth S. Plante, Alan C. Whitmore, Colton L. Linnertz, Emily A. Madden, Kelsey E. Noll, Samuel P. Boyson, Breantie Parotti, James G. Xenakis, Timothy A. Bell, Pablo Hock, Ginger D. Shaw, Fernando Pardo-Manuel de Villena, Martin T. Ferris, Mark T. Heise.

References

1. Gnjatic S, Bronte V, Brunet LR, Butler MO, Disis ML, Galon J, et al. Identifying baseline immune-related biomarkers to predict clinical outcome of immunotherapy. J Immunother Cancer. 2017; 5: 44. https://doi.org/10.1186/s40425-017-0243-4 PMID: 28515944
2. Graham JB, Swarts JL, Menachery VD, Gralinski LE, Schäfer A, Plante KS, et al. Immune Predictors of Mortality After Ribonucleic Acid Virus Infection. J Infect Dis. 2020; 221(6):882–889. https://doi.org/10.1093/infdis/jiz531 PMID: 31621854
3. HIPC-CHI Signatures Project Team; HIPC-I Consortium. Multicohort analysis reveals baseline transcriptional predictors of influenza vaccination responses. Sci Immunol. 2017; 2(14):eaal4656. https://doi.org/10.1126/sciimmunol.aal4656 PMID: 28842433
4. Tsang JS, Schwartzberg PL, Kotliarov Y, Biancotto A, Xie Z, Germain RN, et al. Global analyses of human immune variation reveal baseline predictors of postvaccination responses. Cell. 2014; 157 (2):499–513. https://doi.org/10.1016/j.cell.2014.03.031 PMID: 24725414
5. Crimeen-Irwin B, Scalzo K, Gloster S, Mottram PL, Pleblanski M. Failure of immune homeostasis—the consequences of under and over reactivity. Curr Drug Targets Immune Endocr Metabol Disord. 2005; 5 (4):413–422. https://doi.org/10.2174/156800805774912980 PMID: 16375694
6. Palma J, Tokarz-Deptula B, Deptula J, Deptula W. Natural antibodies—facts known and unknown. Cent Eur J Immunol. 2018; 43(4):466–475. https://doi.org/10.5114/ceji.2018.81354 PMID: 30799995

7. Graham JB, Swarts JL, Mooney M, Choonoo G, Jeng S, Miller DR, et al. Extensive Homeostatic T Cell Phenotypic Variation within the Collaborative Cross. Cell Rep. 2017; 21(8):2313–2325. https://doi.org/10.1016/j.celrep.2017.10.093 PMID: 29166619

8. Krištić J, Zaytseva OO, Ram R, Nguyen Q, Novokmet M, Vučković F, et al. Profiling and genetic control of the murine immunoglobulin G glycome. Nat Chem Biol. 2018; 14(5):516–524. https://doi.org/10.1038/s41589-018-0034-3 PMID: 29632412

9. Phillippi J, Xie Y, Miller DR, Bell TA, Zhang Z, Lenarcic AB, et al. Using the emerging Collaborative Cross to probe the immune system. Genes Immun. 2014; 15(1):38–46. https://doi.org/10.1038/gene.2013.59 PMID: 24195963

10. Collin R, Balmer L, Moraham G, Lesage S. Common Heritable Immunological Variations Revealed in Genetically Diverse Inbred Mouse Strains of the Collaborative Cross. J Immunol. 2019; 202(3):777–786. https://doi.org/10.4049/jimmunol.1801247 PMID: 30587532

11. Cassidy JT, Nordby GL, Dodge HJ. Biologic variation of human serum immunoglobulin concentrations: sex-age specific effects. J Chronic Dis. 1974; 27(11–12):507–516. https://doi.org/10.1016/0021-9681(74)90026-5 PMID: 4215824

12. Grundbacher FJ. Heritability estimates and genetic and environmental correlations for the human immunoglobulins G, M, and A. Am J Hum Genet. 1974; 26(1):1–12. PMID: 4204534

13. Poon MML, Byington E, Meng W, Kutoba M, Matsumoto R, Grifnoi A, et al. Heterogeneity of human anti-viral immunity shaped by virus, tissue, age, and sex. Cell Rep. 2021; 37(9):110071. https://doi.org/10.1016/j.celrep.2021.110071 PMID: 34852222

14. Collaborative Cross Consortium. The genome architecture of the Collaborative Cross mouse genetic reference population. Genetics. 2012; 190(2):389–401. https://doi.org/10.1534/genetics.111.132639 PMID: 22345608

15. Threadgill DW, Miller DR, Churchill GA, de Villena FP. The collaborative cross: a recombinant inbred mouse population for the systems genetic era. ILAR J. 2011; 52(1):24–31. https://doi.org/10.1093/ilar.52.1.24 PMID: 21411855

16. Welsh CE, Miller DR, Manly KF, Wang J, McMillan L, Morahan G, et al. Status and access to the Collaborative Cross population. Mamm Genome. 2012; 23(9–10):706–712. https://doi.org/10.1007/s00335-012-9410-6 PMID: 22847377

17. Roberts A, Pardo-Manuel de Villena F, Wang W, McMillan L, Threadgill DW. The polymorphism architecture of mouse genetic resources elucidated using genome-wide resequencing data: implications for QTL discovery and systems genetics. Mamm Genome. 2007; 18(6–7):473–481. https://doi.org/10.1007/s00335-007-9045-1 PMID: 17674098

18. Ferris MT, Aylor DL, Bottomly D, Whitmore AC, Aicher LD, Bell TA, et al. Modeling host genetic regulation of influenza pathogenesis in the collaborative cross. PLoS Pathog. 2013; 9(2):e1003196. https://doi.org/10.1371/journal.ppat.1003196 PMID: 23468633

19. He L, Wang P, Schick SF, Huang A, Jacob P 3rd, Yang X, et al. Genetic background influences the effect of thirdhand smoke exposure on anxiety and memory in Collaborative Cross mice. Sci Rep. 2021; 11(1):13285. https://doi.org/10.1038/s41598-021-92702-1 PMID: 34168244

20. Graham JB, Swarts JL, Leist SR, Schäfer A, Menachery VD, Gralinski LE, et al. Baseline T cell immune phenotypes predict virologic and disease control upon SARS-CoV infection in Collaborative Cross mice. PLoS Pathog. 2021; 17(1):e1009287. https://doi.org/10.1371/journal.ppat.1009287 PMID: 33513210

21. Gu B, Shorter JR, Williams LH, Bell TA, Hock P, Dalton KA, et al. Collaborative Cross mice reveal extreme epilepsy phenotypes and genetic loci for seizure susceptibility. Epilepsia. 2020; 61(9):2010–2021. https://doi.org/10.1111/epi.16617 PMID: 32852103

22. Smith CM, Proulx MK, Lai R, Kiristsy MC, Bell TA, Hock P, et al. Functionally Overlapping Variants Control Tuberculosis Susceptibility in Collaborative Cross Mice. mBio. 2019; 10(6):e02791–19. https://doi.org/10.1128/mBio.02791-19 PMID: 31772048

23. Noll KE, Whitmore AC, West A, McCarthy MK, Morrison CR, Plante KS, et al. Complex Genetic Architecture Underlies Regulation of Influenza-A-Virus-Specific Antibody Responses in the Collaborative Cross. Cell Rep. 2020; 31(4):107587. https://doi.org/10.1016/j.celrep.2020.107587 PMID: 32348764

24. Hampton BK, Jensen KL, Whitmore AC, Linnertz CL, Maurizio P, Miller DR, et al. Genetic regulation of homeostatic immune architecture in the lungs of collaborative cross mice. BioRxiv [Preprint]. bioRxiv 2021.04.09.439180: Available from: https://www.biorxiv.org/content/10.1101/2021.04.09.439180v1 https://doi.org/10.1101/2021.04.09.439180

25. Morgado MG, Cam P, Gris-Liebe C, Cazenave PA, Jouvin-Marche E. Further evidence that BALB/c and C57BL/6 gamma 2a genes originate from two distinct isotypes. EMBO J. 1989; 8(11):3245–3251. https://doi.org/10.1002/j.1460-2075.1989.tb08484.x PMID: 2510996

26. Zhang Z, Goldschmidt T, Salter H. Possible allelic structure of IgG2a and IgG2c in mice. Mol Immunol. 2012; 50(3):169–171. https://doi.org/10.1016/j.molimm.2011.11.006 PMID: 22177661

27. Srivastava A, Morgan AP, Najarian ML, Sarsani VK, Sigmon JS, Shorter JS, et al. Genomes of the Mouse Collaborative Cross. Genetics. 2017; 206(2):537–556. https://doi.org/10.1534/genetics.116.198838 PMID: 28592495

28. Shorter JR, Najarian ML, Bell TA, Blanchard M, Ferris MT, Hock P, et al. Whole Genome Sequencing and Progress Toward Full Inbreeding of the Mouse Collaborative Cross Population. G3 (Bethesda). 2019; 9(5):1303–1311. https://doi.org/10.1534/g3.119.400039 PMID: 30858237

29. Keele GR, Quach BC, Israel JW, Chappell GA, Lewis L, Safi A, et al. Integrative QTL analysis of gene expression and chromatin accessibility identifies multi-tissue patterns of genetic regulation. PLoS Genet. 2020; 16(1):e1008537. https://doi.org/10.1371/journal.pgen.1008537 PMID: 31961859

30. Keane TM, Goodstadt L, Danecek P, White MA, Wong K, Yalcin B, et al. Mouse genomic variation and its effect on phenotypes and gene regulation. Nature. 2011; 477(7364):289–294. https://doi.org/10.1038/nature10413 PMID: 21921910

31. Doran AG, Wong K, Flint J, Adams DJ, Hunter KW, Keane TM. Deep genome sequencing and variation analysis of 13 inbred mouse strains defines candidate phenotypic alleles, private variation and homozygous truncating mutations. Genome Biol. 2016; 17(1):167. https://doi.org/10.1186/s13059-016-1024-y PMID: 27480531

32. Waterfield M, Khan IS, Cortez JT, Fan U, Metzger T, Greer A, et al. The transcriptional regulator Aire coopts the repressive ATF7ip-MBD1 complex for the induction of immunotolerance. Nat Immunol. 2014; 15(3):258–265. https://doi.org/10.1038/ni.2820 PMID: 24464130

33. Lax E, Sapozhnikov DM. Adult Neural Stem Cell Multipotency and Differentiation Are Directed by the Methyl-CpG-Binding Protein MBD1. J Neurosci. 2017; 37(16):4228–4230. https://doi.org/10.1523/JNEUROSCI.0411-17.2017 PMID: 28424299

34. Jobe EM, Gao Y, Eisinger BE, Mladucky JK, Giuliani CC, Kelnhofer LE, et al. Methyl-CpG-Binding Protein MBD1 Regulates Neuronal Lineage Commitment through Maintaining Adult Neural Stem Cell Identity. J Neurosci. 2017; 37(3):523–536. https://doi.org/10.1523/JNEUROSCI.1075-16.2016 PMID: 28100736

35. Matsumara Y, Nakaki R, Inagaki T, Yoshida A, Kano Y, Kimura H, et al. H3K4/H3K9me3 Bivalent Chromatin Domains Targeted by Lineage-Specific DNA Methylation Pauses Adipocyte Differentiation. Mol Cell. 2015; 60(4):584–596. https://doi.org/10.1016/j.molcel.2015.10.025 PMID: 26590716

36. Zhao X, Ueba T, Christie BR, Barkho B, McConnell MJ, Nakashima K, et al. Mice lacking methyl-CpG binding protein 1 have deficits in adult neurogenesis and hippocampal function. Proc Natl Acad Sci U S A. 2003; 100(11):6777–6782. https://doi.org/10.1073/pnas.1131928100 PMID: 12748381

37. Kapellos TS, Bonaguro L, Gemünd I, Reusch N, Saglam A, Hinkley ER, et al. Human Monocyte Subsets and Phenotypes in Major Chronic Inflammatory Diseases. Front Immunol. 2019; 10:2035. https://doi.org/10.3389/fimmu.2019.02035 PMID: 31543877

38. Smeester L, Bommarito PA, Martin EM, Recio-Vega R, Gonzalez-Corets T, Olivas-Calderon E, et al. Chronic early childhood exposure to arsenic is associated with a TNF-mediated proteomic signaling response. Environ Toxicol Pharmacol. 2017; 52:183–187. https://doi.org/10.1016/j.etap.2017.04.007 PMID: 28433805

39. Falk I, Potocnik AJ, Barthlott T, Levelt CN, Elchmann K. Immature T cells in peripheral lymphoid organs of recombinase-activating gene-1/-2-deficient mice. Thymus dependence and responsiveness to anti-CD3 epsilon antibody. J Immunol. 1996; 156(4):1362–1368. PMID: 8568235

40. Kitamura D, Roes J, Kühn R, Rajewsky K. A B cell-deficient mouse by targeted disruption of the membrane exon of the immunoglobulin mu chain gene. Nature. 1991; 350(6317):423–426. https://doi.org/10.1038/350423a0 PMID: 1901381

41. Lansford R, Manis JP, Sonoda E, Rajewsky K, Alt FW. Ig heavy chain class switching in Rag-deficient mice. Int Immunol. 1998; 10(3):325–332. https://doi.org/10.1093/intimm/10.3.325 PMID: 9576620

42. Khattri R, Kasprowicz D, Cox T, Mortrud M, Appleby MW, Brunkow ME, et al. The amount of scurfin protein determines peripheral T cell number and responsiveness. J Immunol. 2001; 167(11):6312–6320. https://doi.org/10.4049/jimmunol.167.11.6312 PMID: 11714795

43. Kasprowicz DJ, Smallwood PS, Tyznik AJ, Ziegler SF. Scurfin (FoxP3) controls T-dependent immune responses in vivo through regulation of CD4+ T cell effector function. J Immunol. 2003; 171(3):1216–1223. https://doi.org/10.4049/jimmunol.171.3.1216 PMID: 12874208

44. Collins AM. IgG subclass co-expression brings harmony to the quartet model of murine IgG function. Immunol Cell Biol. 2016; 94(10):949–954. https://doi.org/10.1038/icb.2016.65 PMID: 27502143

45. Vidarsson G, Dekkers G, Rispen T. IgG subclasses and allotypes: from structure to effector functions. Front Immunol. 2014; 5:520. https://doi.org/10.3389/fimmu.2014.00520 PMID: 25368619

46. Smith CM, Proulx MK, Olive AJ, Laddy D, Mishra BB, Moss C, et al. Tuberculosis Susceptibility and Vaccine Protection Are Independently Controlled by Host Genotype. mBio. 2016; 7(5):e01516–16. https://doi.org/10.1128/mBio.01516-16 PMID: 27651361

47. Petruchina I, Tran M, Sadzikava N, Ghochikyan A, Vasilevko V, Agadjanyan MG, et al. Importance of IgG2c isotype in the immune response to beta-amyloid in amyloid precursor protein/transgenic mice. Neurosci Lett. 2003; 338(1):5–8. https://doi.org/10.1016/s0304-3940(02)01357-5 PMID: 12565127

48. Holodick NE, Rodriguez-Zhurbenko N, Hernandez AM. Defining Natural Antibodies. Front Immunol. 2017; 8:872. https://doi.org/10.3389/fimmu.2017.00872 PMID: 28798747

49. Zhou ZH, Zhang Y, Hu YF, Wahl LM, Cisar JO, Notkins AL. The broad antibacterial activity of the natural antibody repertoire is due to polyreactive antibodies. Cell Host Microbe. 2007; 1(1):51–61. https://doi.org/10.1016/j.chom.2007.01.002 PMID: 18005681

50. Subramaniam KS, Datta K, Quintero E, Manix C, Marks MS, Pirofski LA. The absence of serum IgM enhances the susceptibility of mice to pulmonary challenge with Cryptococcus neoformans. J Immunol. 2010; 184(10):5755–5767. https://doi.org/10.4049/jimmunol.0901638 PMID: 20404271

51. Jayasekera JP, Moseman EA, Carroll MC. Natural antibody and complement mediate neutralization of influenza virus in the absence of prior immunity. J Virol. 2007; 81(7):3487–3494. https://doi.org/10.1128/JVI.02128-06 PMID: 17202212

52. Panda S, Ding JL. Natural antibodies bridge innate and adaptive immunity. J Immunol. 2015; 194 (1):13–20. https://doi.org/10.4049/jimmunol.1400844 PMID: 25527792

53. New JS, King RG, Kearney JF. Manipulation of the glycan-specific natural antibody repertoire for immunotherapy. Immunol Rev. 2016; 270(1):32–50. https://doi.org/10.1111/imr.12397 PMID: 26864103

54. Fujita N, Shimotake N, Ohki I, Chiba T, Saya H, Shirakawa M, et al. Mechanism of transcriptional regulation by methyl-CpG binding protein MBD1. Mol Cell Biol. 2000; 20(14):5107–5118. https://doi.org/10.1128/MCB.20.14.5107-5118.2000 PMID: 10866667

55. Ichimura T, Watanabe S, Sakamoto Y, Aoto T, Fujita N, Makao M. Transcriptional repression and heterochromatin formation by MBD1 and MCAF/AM family proteins. J Biol Chem. 2005; 280(14):13928–13935. https://doi.org/10.1074/jbc.M413654200 PMID: 15691849

56. Herviou L, Jourdan M, Martinez A, Cavalli G, Moreaux J. EZH2 is overexpressed in transitional preplasmablasts and is involved in human plasma cell differentiation. Leukemia. 2019; 33(8):2047–2060. https://doi.org/10.1038/s41375-019-0392-1 PMID: 30755708

57. Haines RR, Barwick BG, Scharer CD, Majumber P, Randall TD, Boss JM. The Histone Demethylase LSD1 Regulates B Cell Proliferation and Plasmablast Differentiation. J Immunol. 2018; 201(9):2799–2811. https://doi.org/10.4049/jimmunol.1800952 PMID: 30232138

58. Barwick BG, Scharer CD, Bally APR, Boss JM. Plasma cell differentiation is coupled to division-dependent DNA hypomethylation and gene regulation. Nat Immunol. 2016; 17(10):1216–1225. https://doi.org/10.1038/ni.3519 PMID: 27500631

59. Barwick BG, Scharer CD, Martinez RJ, Price MJ, Wein AN, Haines RR, et al. B cell activation and plasma cell differentiation are inhibited by de novo DNA methylation. Nat Commun. 2018; 9(1):1900. https://doi.org/10.1038/s41467-018-04234-4 PMID: 29765016

60. Gatti DM, Svenson KL, Shabalin A, Wu L, Valdar W, Simecek P, et al. Quantitative trait locus mapping methods for diversity outbred mice. G3 (Bethesda). 2014; 4(9):1623–1633. https://doi.org/10.1534/g3.114.013748 PMID: 25237114